Parasitol Res (2014) 113:81–90
DOI 10.1007/s00436-013-3629-3

ORIGINAL PAPER

Morphology and 18S rDNA sequencing identifies *Henneguya visibilis* n. sp., a parasite of *Leporinus obtusidens* from Mogi Guaçu River, Brazil

Gabriel S. A. Moreira · Edson A. Adriano · Marcia R. M. Silva · Paulo S. Ceccarelli · Antônio A. M. Maia

Received: 2 April 2013 / Accepted: 26 September 2013 / Published online: 8 October 2013

Abstract During a survey of myxozoan parasites of freshwater fish from the Mogi Guaçu River in São Paulo State, Brazil, plasmodia of *Henneguya visibilis* n. sp. were found on the fins of *Leporinus obtusidens* (Characiformes: Anostomidae). The plasmodia, which were observed on five out of eight (62.5 %) *L. obtusidens* examined, were 400–1,000 μm long. Mature spores were elongated with a spore body 10.8±0.6 μm long and 3.9±0.2 μm wide, a caudal process 18±1.2 μm long, and a total spore length of 26.8±1.1 μm. Polar capsules were elongated 4.9±0.3 μm long and 1.4±0.1 μm wide. Histological examination indicated that the plasmodia developed in the connective tissue, and no inflammatory infiltrate was observed at the infection site. Ultrastructural analysis showed a plasmodium wall with a single membrane and several pinocytotic canals. Sporogenesis occurred from the periphery to the center of the plasmodia. Phylogenetic analysis of the 18S rDNA sequence using maximum likelihood and maximum parsimony methods showed *H. visibilis* n. sp. positioned in a sub-clade composed of *Henneguya/Myxobolus* parasites of several freshwater fish families.

G. S. A. Moreira · M. R. M. Silva · A. A. M. Maia
Departamento de Medicina Veterinária, Faculdade de Zootecnia e Engenharia de Alimentos, Universidade de São Paulo (USP), Rua Duque de Caxias Norte, 225, Pirassununga, São Paulo 13635-900, Brazil

G. S. A. Moreira
e-mail: gabrielmoreira@usp.br

M. R. M. Silva
e-mail: marciamg@usp.br

A. A. M. Maia
e-mail: antomaia@usp.br

E. A. Adriano (✉)
Departamento de Ciências Biológicas, Universidade Federal de São Paulo (Unifesp), Rua Professor Artur Riedel, 275, Jardim Eldorado, Diadema, São Paulo 09972-270, Brazil
e-mail: edapadriano@gmail.com

E. A. Adriano
Departamento de Biologia Animal, Instituto de Biologia, Universidade Estadual de Campinas (UNICAMP), Caixa Postal 6109, Campinas, São Paulo 13083-970, Brazil

P. S. Ceccarelli
Centro Nacional de Pesquisa e Conservação de Peixes Continentais (CEPTA), Instituto Chico Mendes de Conservação da Biodiversidade (ICMBio), Rod. SP 201, Km 6.5, Caixa Postal 64, Pirassununga, São Paulo 13630-970, Brazil
e-mail: paulo.ceccarelli@icmbio.gov.br

Introduction

Myxozoans are among the most common fish parasites (Feist and Longshaw 2006; Fleurance et al. 2008), with more than 2,180 known species (Morris 2010). They are known to primarily infect marine and freshwater fish (Lom and Dykova 2006) but have also been observed infecting amphibians, reptiles, birds, and mammals (Bartholomew et al. 2008). *Henneguya* spp. are myxozoan parasites within the family Myxobolidae, of which there are more than 194 known species (Eiras and Adriano 2012). Of these known species, 43 have been described in South American fish (Azevedo et al. 2009; Adriano et al. 2012), 6 of which were wild Anostomid fishes: *Henneguya leporini* Nemeczek, 1926, a parasite of *Leporinus mormyrops*; *Henneguya schizodon* Eiras et al., 2004, from *Schizodon fasciatus*; *Henneguya caudicula* Eiras et al., 2008, from *Leporinus lacustris*; *Henneguya friderici* Casal et al., 2003, from *Leporinus friderici*; and *Henneguya azevedoi* Barassa et al., 2012, from *Leporinus obtusidens* (Nemeczek 1926; Eiras 2002; Eiras et al. 2004, 2008; Casal et al. 2003; Barassa et al. 2012). In addition, *Henneguya leporinicola* Martins et al., 1999, has been reported from cultured *Leporinus macrocephalus* (Martins et al. 1999).

L. obtusidens Valenciennes, 1837, is a rheophilic omnivorous fish of the family Anostomidae that possesses many names. The distribution of *L. obtusidens*, known as *piapara*, *piaba*, or *piava* in Portuguese, *boga* or *bogón* in Spanish, and *characin* in English (Froese and Pauly 2012), is restricted to the basins of the La Plata and São Francisco Rivers in Brazil (Froese and Pauly 2012; Santos 2000). As part of a continuous investigation into the biodiversity of myxozoan parasites of freshwater fishes in Brazil, a new species of *Henneguya* was found infecting the fins of several *L. obtusidens* from the Mogi Guaçu River in the upper Paraná River Basin. The present study characterizes this new myxozoan taxon using morphological, histological, ultrastructural, and molecular data.

Materials and methods

Eight *L. obtusidens* specimens were caught downstream of the Cachoeira de Emas power plant (21°55′37″ S, 47°22′03″ W) in the Mogi Guaçu River, located in the Paraná River Basin in the Pirassununga municipality of the state of São Paulo, Brazil. The fish were caught using cast nets from April 2011 to August 2011. After capture, the fish were transported alive to the laboratory, where they were euthanized by benzocaine overdose in accordance with Brazilian law (Federal Law No. 11.794, of 8 October 2008 and Federal Decree No. 6899, of 15 July 2009). The fish were then measured and necropsied. Mature parasitic spores were examined on fresh wet mounts by light microscopy. Morphological and morphometric analysis was performed on mature spores ($n=30$) obtained from different plasmodia based on the criteria outlined by Lom and Arthur (1989).

For histological analysis, fragments of the infected organs were fixed in 10 % buffered formalin for 24 h, dehydrated in 70 and 95 % ethyl alcohol for 1 h each, dehydrated in 100 % alcohol twice for 1 h each step, and incubated twice in xylene for 1 h each. The fragments were then embedded in paraffin, cut into serial sections 6 μm thick, and stained with hematoxylin/eosin.

For transmission electron microscopy, plasmodia were fixed with 2.5 % glutaraldehyde in 0.1 M cacodylate buffer (pH 7.4) for 12 h, washed in a glucose–saline solution for 2 h, and postfixed in OsO_4. All of these steps were performed at 4 °C. After dehydration using an acetone series, the material was embedded in an EMbed 812 resin (Electron Microscopy Sciences, Hatfield, PA, USA). Ultrathin sections that were dual stained with uranyl acetate and lead citrate were examined using an LEO 906 electron microscope operated at 60 kV.

For the molecular study, pooled plasmodia were collected in a 1.5-ml microcentrifuge tube, and DNA was extracted using a DNeasy® Blood & Tissue Kit (Qiagen) according to the manufacturer's instructions. The DNA concentration was determined using a NanoDrop 2000 spectrophotometer (Thermo Scientific, Wilmington, DE, USA) at 260 nm. Polymerase chain reaction (PCR) was conducted in a final volume of 25 μl, and the reaction contained 10–50 ng of extracted DNA, 1× Taq DNA polymerase buffer (Invitrogen by Life Technologies, Brazil), 0.2 mmol of dNTPs, 1.5 mmol of $MgCl_2$, 0.5 pmol of each primer, 1.25 U of Taq DNA polymerase (Invitrogen by Life Technologies, MD, USA), and ultrapure water (Barnstead/Thermolyne, Dubuque, IA, USA). PCR was performed with an AG 22331 Hamburg Thermocycler (Eppendorf, Hamburg, Germany). Fragments of approximately 850 and 1,200 bp were amplified using the primer pairs HenBr-F–HenBr-R (designed during this study) and the Myxgen4F–Erib10 (Table 1).

Initial denaturation was performed at 95 °C for 5 min, followed by 35 cycles of denaturation (95 °C for 60 s), annealing (58 °C for 60 s), and extension (72 °C for 90 s) and a final extended elongation step at 72 °C for 5 min. PCR products were electrophoresed using a 1.0 % agarose gel (BioAmerica, Miami, FL, USA) in TAE buffer (0.045 M Tris–borate, 0.001 M EDTA; pH 8.0), stained with ethidium bromide and analyzed using a FLA-3000 scanner (Fuji Photo Film, Tokyo, Japan). The size of the amplified fragments was estimated by comparison with a 1-kb DNA ladder (Invitrogen by Life Technologies, CA, USA). The PCR product obtained from *Henneguya* was purified and sequenced using the same primer pairs used for amplification in addition to the MC5–MC3 primer pair (Table 1).

Sequencing was performed using the BigDye® Terminator v3.1 cycle sequencing kit (Applied Biosystems Inc., CA, USA) with an ABI 3730 DNA sequencing analyzer (Applied Biosystems). A standard nucleotide BLAST (blastn) search was then conducted (Altschul et al. 1997). The BioEdit program (Hall 1999) was used to align the sequences obtained and compare them with sequences deposited in GenBank.

Phylogenetic analysis was conducted using the obtained 18S rDNA (1,710 bp) sequence of the case isolate, as well as representative sequences from species of *Myxobolus/Henneguya* available in GenBank. Analysis was performed using 56 *Henneguya* and *Myxobolus* spp. sequences representing parasites of several orders and/or families of host fish (Rosenberg and Kumar 2001). Two species of the genus *Ceratomyxa* (*Ceratomyxa shasta* and *Ceratomyxa sparusaurati*) were chosen as an outgroup due to their evolutionary distance from *Myxobolus* and *Henneguya* (Fiala 2006; Easy et al. 2005; Molnár et al. 2006; Milanin et al. 2010; Naldoni et al. 2011).

To ensure the accuracy of the analysis and maintain a high tree resolution, sequences shorter than 1,000 bp were not used, avoiding the loss of information due to shortening of the aligned sequences and the appearance of numerous gaps, as previously observed (Liu et al. 2010). ClustalW (Thompson et al. 1997) in BioEdit was used to adjust the alignments. The total alignment, with 2,223 informative characters of 18S rDNA, was used for phylogenetic analyses. The jModelTest

Table 1 Primes utilized at the amplification and sequencing of the 18S rDNA gene

Primers	Sequences	Reference
HenBr-F (forward)	5′-GTTATTGGATAACCGTGGGAAATCT-3′	This study
HenBr-R (reverse)	5′-ACGATTGTTCGTTCCATGCTA-3′	This study
MYXGEN4F (forward)	5′-GTGCCTTGAATAAATCAGAG-3′	Diamant et al. (2004)
ERIB10 (reverse)	5′-CTTCCGCAGGTTCACCTACGG-3′	Barta et al. (1997)
MC5 (forward)	5′-CCTGAGAAACGGCTACCACATCCA-3′	Molnár et al. (2002)
MC3 (reverse)	5′-GATTAGCCTGACAGATCACTCCACGA-3′	Molnár et al. (2002)

0.1 program (Posada 2008) was used to determine the best evolution model. The GTR + I + G model was selected with nucleotide frequencies (A=0.2472, C=0.1826, G=0.2747, and T=0.2955) and six rates of nucleotide substitution (AC=0.9692, AG=3.0930, AT=1.2936, CG=0.6382, CT=3.9541, and GT=1.0000). The proportion of invariable sites was 0.0580, and the gamma shape was 0.3750. These parameters were then used for maximum likelihood (ML) analysis, which was performed using PhyML 3.0 (Guindon et al. 2010). For the maximum parsimony (MP) analysis, the PAUP* 4.0b10 program (Swofford 2003) was used. Bootstrap analysis with 100 replicates in ML and 1,000 in MP was employed to assess the relative robustness of the tree branches. The tree was initially examined in FigTree v1.3.1 (Rambaut 2009) and edited and annotated in Adobe Illustrator (Adobe Systems Inc. San Jose, CA, USA). Based on the results of the phylogenetic analyses, a second alignment including only the *Myxobolus*/*Henneguya* species closest to the species described here was used to evaluate the genetic distance, which was performed using the pairwise method with the p-distance model using MEGA 5.0 (Tamura et al. 2011).

Results

Description of *Henneguya visibilis* n. sp.

- Vegetative stages: Plasmodia white and elongated, 400–1,000 μm long, located in the connective tissue near the fin rays. Histological analysis showed plasmodia surrounded by a thin layer of connective tissue, and the growth of the plasmodia led to mild compression on adjacent tissue. No inflammatory infiltrate was observed (Figs. 1, 2, and 3).
- Mature spores: Spores ellipsoidal in the frontal view and biconvex laterally, 26.8±1.1 μm in total length, 10.8±0.6 μm in body length, 3.9±0.2 μm wide, and with 18±1.2 μm caudal process. Polar capsules elongated, 4.9±0.3 μm long, and 1.4±0.1 μm wide (Fig. 1) (Table 2). Ultrastructural analysis indicated plasmodia with a single membrane and several pinocytotic canals that connected the outside of the plasmodium to the ectoplasm (Figs. 4 and 5). Just below the ectoplasm, mitochondria and numerous immature and mature spores were observed in the central area of the plasmodia (Figs. 4 and 5). Sections of the young spores indicated a polar capsule with eight to nine coils positioned obliquely to the longitudinal axis of the capsule and binucleated sporoplasms that contained few sporoplasmosomes (Figs. 6–9).
- Type host: *L. obtusidens* (Valenciennes, 1837) (Osteichthyes, Anostomidae).
- Site of infection: Connective tissue of the fins.
- Prevalence: Of eight fish examined, five were infected (62.5 %).
- Locality: The Mogi Guaçu River is in close proximity to the Cachoeira de Emas Falls (21°55′37″ S, 47°22′03″ W), Pirassununga, state of São Paulo, Brazil.
- Material type: One slide containing free spores fixed with methanol, stained with Giemsa solution, and mounted using a low-viscosity mounting medium was deposited in the Museum of Natural History, Institute of Biology, State University of Campinas, São Paulo State, Brazil (accession no. ZUEC MYX 33).
- Etymology: The specific name "*visibilis*" refers to the easy visualization of the plasmodia and is derived from the Latin *visibilis*, meaning visible.

Sequencing of the 18S rDNA gene from spores of *H. visibilis* n. sp. resulted in a partial sequence of 1,710 bp (GenBank accession number KC771143). The most similar sequences identified by a blastn search were *Henneguya sutherlandi* and *Henneguya pellis* from ictalurid fishes in the USA and *Myxobolus oliveirai* from characid fishes in Brazil.

The analysis of the genetic distance shows that the closest species to *H. visibilis* n. sp. were *Henneguya eirasi* HQ655111 (15.3 %), *H. sutherlandi* EF191200 (15.9 %), and *H. pellis* FJ468488 (16 %).

Phylogenetic analyses using ML and MP methods showed that *Henneguya* and *Myxobolus* species clustered into three clades (Fig. 10). Basal clade A harbored exclusively *Myxobolus* spp. of salmoniforms. Clade B further divided to form sub-clade B1 which clustered *Henneguya* spp. parasites of marine fish from Perciformes. Sub-clade B2 further divided

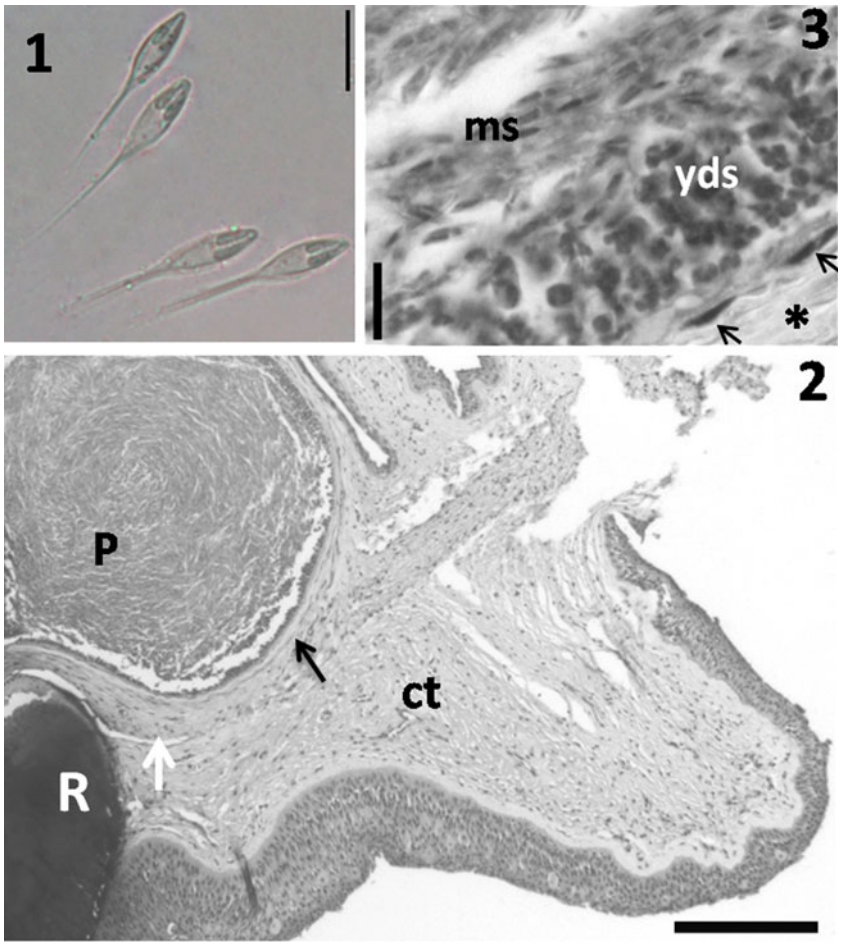

Figs. 1–3 Light photomicrographs of *H. visibilis* n. sp. *1* Fresh preparation showing two mature spores. *Scale bar* = 10 μm. *2* Histological sections of the fin of *L. obtusidens* showing a plasmodium (*P*) in the connective tissues (*ct*) near the ray (*R*). Note the capsule of connective tissue (*black arrow*) surrounding the plasmodium and a weak compression of the adjacent tissues (*white arrow*). *Scale bar* = 200 μm. *3* Amplified section of *2* showing the capsule of connective tissue (*asterisk*) with fibroblast nuclei (*arrows*) in the region nearest to the plasmodia. Inside, note the peripheral zone with young developmental stages (*yds*) and mature spores (*ms*) in the central zone. *Scale bar* = 10 μm

to form sub-clade B2a, which harbored *Myxobolus* spp. parasites of mugiliforms, and sub-clade B2b, which clustered parasites of several freshwater fish families, including *H. visibilis* n. sp. Clade C was formed by *Henneguya*/*Myxobolus* parasite species of Salmoniformes, Cypriniformes, and Siluriformes.

Discussion

The morphological characteristics of *H. visibilis* n. sp. were compared with those of all the *Henneguya* species reported to infect South American freshwater fish, as well as fish parasites from other regions (Eiras 2002; Eiras and Adriano 2012). Among the 43 *Henneguya* species found in South American freshwater fish, the following 6 have been described to infect fish of the family Anostomidae: *H. schizodon* infects the kidney of *S. fasciatus*, *H. leporinicola* is a parasite of the gills of *L. macrocephalus*, *H. leporini* is a parasite of the urinary ducts of *L. mormyrops*, *H. friderici* infects the gills of *L. friderici*, *H. caudicula* is a parasite of the gills of *L. lacustris*, and *H. azevedoi* is a parasite of the gills of *L. obtusidens* (Barassa et al. 2012; Eiras 2002; Eiras and Adriano 2012).

The morphological comparison of *H. visibilis* n. sp. with parasite species of anostomid fishes indicated that the spores of *H. visibilis* n. sp. were more similar to those of *H. schizodon* with regard to dimensions of total spore length (28.6 μm in *H. schizodon* and 26.8±1.1 μm in *H. visibilis* n. sp.), body width (3.3 μm in *H. schizodon* and 3.9±0.2 μm in *H. visibilis* n. sp.), capsule length (5.4 μm in *H. schizodon* and 4.9±0.3 μm in *H. visibilis* n. sp.), capsule width (1.3 μm in *H. schizodon* and 1.4±0.1 μm in *H. visibilis* n. sp.), and polar turns (eight to ten in *H. schizodon* and eight to nine in *H. visibilis* n. sp.).

Although there are no 18S rDNA gene data of *H. schizodon* to compare with *H. visibilis* n. sp., morphological differences, including those related to the spore body length (13.1 μm for *H. schizodon* and 10.8±0.6 μm for *H. visibilis* n. sp.), length and format of the tail (*H. schizodon*, bifurcate near the spore body and 16.3 μm long; *H. visibilis* n. sp., bifurcate approximately in the middle of the tail and 18±1.2 μm long), and shape and size of the plasmodium (spherical and measuring 250–500 μm for *H. schizodon* and elongated and

Table 2 Measurements, infection sites, and geographic regions of *Henneguya* spp. compared with *H. visibilis* n. sp., a parasite of *L. obtusidens*

Parasite	TL	BL	CA	BW	LC	WC	T	PT	Site of infection	Host	Country
Henneguya visibilis n. sp.	26.8±1.1	10.8±0.6	18±1.2	3.9±0.2	4.9±0.3	1.4±0.1	3.7±0.5	8–9	Fin	*Leporinus obtusidens*	Brazil
Henneguya schizodon Eiras et al., 2004	28.9 (27–30)	13.1 (12–14)	16.3 (15–17)	3.3 (3.4)	5.4 (5–6)	1.3 (1–1.5)	–	8–10	Kidney	*Schizodon fasciatus*	Brazil
Henneguya azevedoi Barassa et al., 2012	45.2 (45.5–47.0)	10.0 (9.9–10.2)	35.6 (34.9–36.5)	4.4 (4.0–5.0)	3.8 (3.5–4.0)	1.0	–	6–7	Gills	*Leporinus obtusidens*	Brazil
Henneguya leporini Nemeczek, 1926	28–33	13–15	15–18	5	5–8	–	–	–	Urinary ducts	*Leporinus mormyrops*	Brazil
Henneguya caudicula Takemoto and Pavanelle, 2008	14.7 (14–16)	11.3 (11–12)	3.6 (3–4)	5.4 (5–6)	3.7 (3–4)	1.5	3.6	3	Gills	*Leporinus lacustris*	Brazil
Henneguya leporinicola Martins et al., 1999	–	7.6 (5.5–8.7)	21.8 (12.9–32.3)	4.2 (3.6–4.9)	3.0 (2.0–3.6)	1.6 (1.2–2.0)	–	–	Gills	*Leporinus macrocephalus*	Brazil
Henneguya friderici Casal et al., 2003	33.8 (28.7–39.9)	10.4 (9.6–11.8)	23.3 (19.1–28.7)	5.7 (4.8–6.6)	4.9 (4.5–5.9)	2.1 (1.5–2.6)	4.9 (4.6–5.2)	7–8	Gills	*Leporinus friderici*	Brazil
Henneguya corruscans Eiras et al., 2009	27.6 (25–29)	14 (13–15)	13.7 (12–15)	5	6.8 (6–7)	2	4	5–6	Gills	*Pseudoplatystoma corruscans*	Brazil
Henneguya adiposa Minchew, 1977	61.0 (45–75)	16.3 (12–19)	44.8 (28–59)	4.0 (2.5–3.5)	7.7 (6.2–9.0)	1.5 (1.0–2.0)	3.0 (2.5–3.5)	6–8	Adipose fin	*Ictalurus punctatus*	USA
Henneguya hainanensis Che and Ma, 1998	24.8 (21.5–30.0)	10.1 (9.5–12.0)	13.0 (12.0–14.4)	4.6 (4.5–4.7)	4.1 (4.0–4.5)	1.6 (1.4–1.8)	3.3 (3.0–3.7)	–	Gills	*Mystus macropterus*	China

TL total length, *BL* body length, *CA* caudal appendage, *BW* body width, *LC* length capsule, *WC* width capsule, *T* thickness, *PT* polar turns

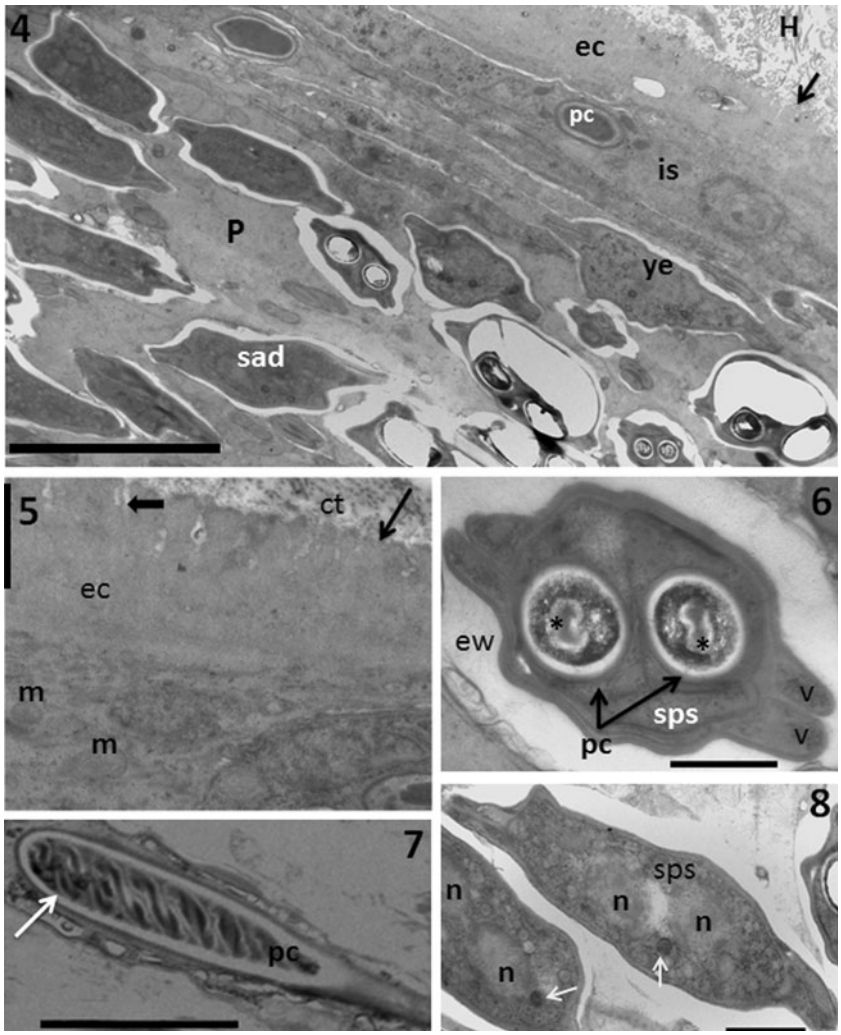

Figs. 4–8 Electron micrography of the fin of *L. obtusidens* infected by *H. visibilis* n. sp. *4* Host–parasite interface showing a broad view of the plasmodium (*P*) and the unique plasmodial wall in direct contact with the connective tissue (*arrow*) of the host (*H*), ectoplasm (*ec*), immature spores (*is*) with unformed polar capsules (*pc*), young spores (*ye*), and spores in advanced developmental stages (*sad*). *Scale bar*=5 μm. *5* Higher magnification showing the plasmodial wall (*thin arrow*) in direct contact with the connective tissue (*ct*), mitochondria (*m*), and pinocytotic canals (*thick arrow*) in the ectoplasm (*ec*). *Scale bar*=1 μm. *6* Transverse sections of a mature spore showing empty white (*ew*) around the spore, the valves (*v*), part of the sporoplasm (*sps*), polar capsules (*pc*), and details of polar filaments (*asterisks*). *Scale bar*=0.5 μm. *7* Longitudinal sections of the spore showing details of polar filament coils (*white arrow*) inside the polar capsule (*pc*). *Scale bar*=2 μm. *8* Transverse section of two immature spores showing the sporoplasms (*sps*) with two nuclei (*n*) and few sporoplasmosomes (*white arrows*). *Scale bar*=1 μm

measuring 400–1,000 μm for *H. visibilis* n. sp.), suggest separating these taxa. Likewise, differences in the host genus of the anostomid family (*Schizodon* for *H. schizodon* and *Leporinus* for *H. visibilis* n. sp.) and tissue predilection (*H. schizodon* in the kidney and *H. visibilis* n. sp. in the fins) are important to support the taxonomic difference. Molnár (1998) suggested that *Henneguya* species may have relatively strict host specificity. Naldoni et al. (2011) and Adriano et al. (2012) corroborated this hypothesis in studies on myxosporeans of the pimelodids *Pseudoplatystoma corruscans*, *Pseudoplatystoma reticulatum*, and *Zungaro jahu* from the Brazilian Pantanal wetland. They found *H. eirasi* and *Henneguya multiplasmodialis* infecting specimens of both species of *Pseudoplatystoma* but not *Z. jahu*, which inhabits the same waters (Naldoni et al. 2011; Adriano et al. 2009, 2012). Geography also plays an important role in the taxonomy of parasites of freshwater fishes because in the freshwater environment, fish species usually live in isolated watersheds. *H. visibilis* n. sp. was found in the La Plata basin, while *H. schizodon* was found in the Amazon basin. The separation of the La Plata and Amazon basins occurred in the Late Miocene in the last 10 Ma (Hubert and Renno 2006), which is a sufficient time for speciation to occur.

Among the *Henneguya* species that infect other families of fish in South America (Eiras 2002; Eiras and Adriano 2012), the most similar to *H. visibilis* n. sp. was *Henneguya corruscans*, a parasite of *P. corruscans* (Eiras et al. 2009), which presented the most similar total spore length (27.6 μm for *H. corruscans* and 26.8±1.1 μm for *H. visibilis* n. sp.). However, they differed in other dimensions, including spore body length (14 μm for *H. corruscans* and 10.8±0.6 μm for *H. visibilis* n. sp.), tail length (13.7 μm in *H. corruscans* and 18±1.2 μm in *H. visibilis* n. sp.), polar capsule length (6.8 μm in *H. corruscans* and 4.9±0.3 μm in *H. visibilis* n. sp.), and the number of polar filament coils (five to six in *H. corruscans* and eight to nine in *H. visibilis* n. sp.). Concerning the 18S rDNA sequence, the distance between the two species was 19 %.

The comparison of *H. visibilis* n. sp. with *Henneguya* spp. around the world indicates that the species described here differs from these other species with regard to at least one of

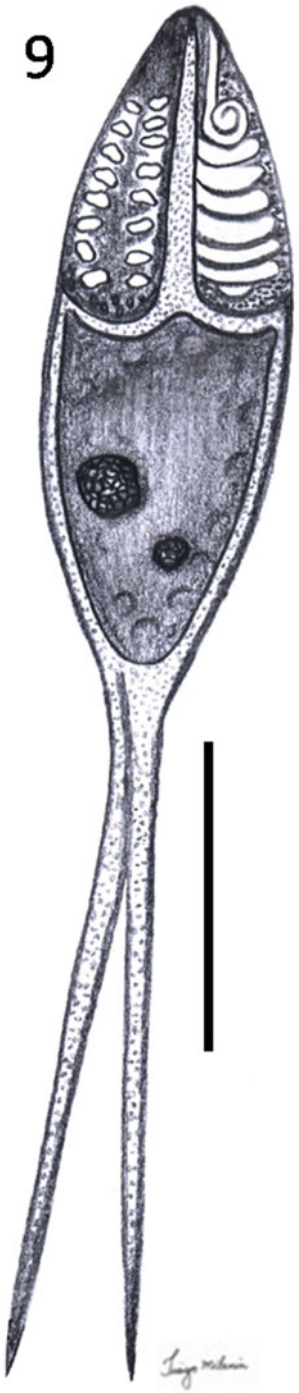

Fig. 9 Schematic representation of mature spores of *H. visibilis* n. sp. from the fins of *L. obtusidens*. *Scale bar* = 5 μm

the following characteristics: plasmodium shape and size, total spore length, spore body length, length of the caudal process, spore width, length or width of polar capsules, number of polar filament turns, infection site, and phylogenetic distance between the hosts (Eiras 2002; Eiras and Adriano 2012). Thus, based on the morphologic, morphometric, and molecular data, site of infection in the host species, and biogeographical aspects, we determined that the parasite studied here is a new myxosporean species.

The plasmodia of *H. visibilis* n. sp. were surrounded by a layer of connective tissue, a common characteristic of myxosporean infection (Sitja-Bobadilla 2008), and the growth of the plasmodia led to mild compression of the adjacent tissues; however, there was no inflammatory infiltrate. A similar presentation has been observed in *Myxobolus portucalensis*, *Myxobolus alburni*, and *Myxobolus caudatus*, whose plasmodia develop in the loose connective tissue layer of skin doublets between the fin rays, and no signs of host reaction are observed around the plasmodia (Molnár 2002).

Ultrastructural data have played an important role in understanding the host–parasite interaction (Current and Janovy 1976; El-Mansy and Bashtar 2002; Adriano et al. 2005a) and have also been used to characterize the sporogenesis of myxosporeans (Morris 2010; Azevedo et al. 2011; Abdel-Ghaffar et al. 2008; Adriano et al. 2005b). Ultrastructural data indicated that the plasmodial wall of *H. visibilis* n. sp. was in direct contact with the connective tissue of the host and the pinocytotic canals linked the outside with the ectoplasm zone. This structure appears to play an important role in supplying the nutrients required for plasmodial development, as previously observed by El-Mansy and Bashtar (2002), Barassa et al. (2012), and Naldoni et al. (2011). The development of *H. visibilis* n. sp. was asynchronic. Numerous mitochondria, generative cells, and young spores were present in the periphery, and mature spores were present in the central area of the plasmodia. This pattern has also been observed in several other myxosporean species (Azevedo et al. 2008; Barassa et al. 2012; Ali et al. 2007; Naldoni et al. 2011).

Iwanowicz et al. (2008) discriminated three distinct diagnostic variable regions (DVR 1 to DVR 3) within the 18S rDNA of the Myxobolidae. In our analysis, the partial sequence of 1,710 bp of the 18S rDNA of *H. visibilis* n. sp. (KC771143) covered half of region DVR 1 and all of regions DVR 2 and DVR 3, corresponding to nucleotides 240–370, 650–960, and 1,500–1,740, respectively. Based on this sequence, the ML and MP phylogenetic analyses indicated that the *Henneguya* and *Myxobolus* species have a strong tendency to form clades based primarily on the environment (marine or freshwater) and order and/or family of the host fish, which confirms the results of Fiala (2006), Ferguson et al. (2008), Khlifa et al. (2012), and Adriano et al. (2012). Those tendencies were observed in almost all clades. Clade A grouped *Myxobolus* spp. parasites exclusively of salmonids and behaved as a basal clade of the others species, while *Henneguya* spp. of salmoniforms clustered in clade C. Clade B harbored two sub-clades composed of species parasites of marine fishes: B1 clustered *Myxobolus* spp. parasites of perciforms and B2a *Henneguya* spp. parasites of mugiliforms. Sub-clade B2b was composed of *Henneguya/Myxobolus* spp. parasites of

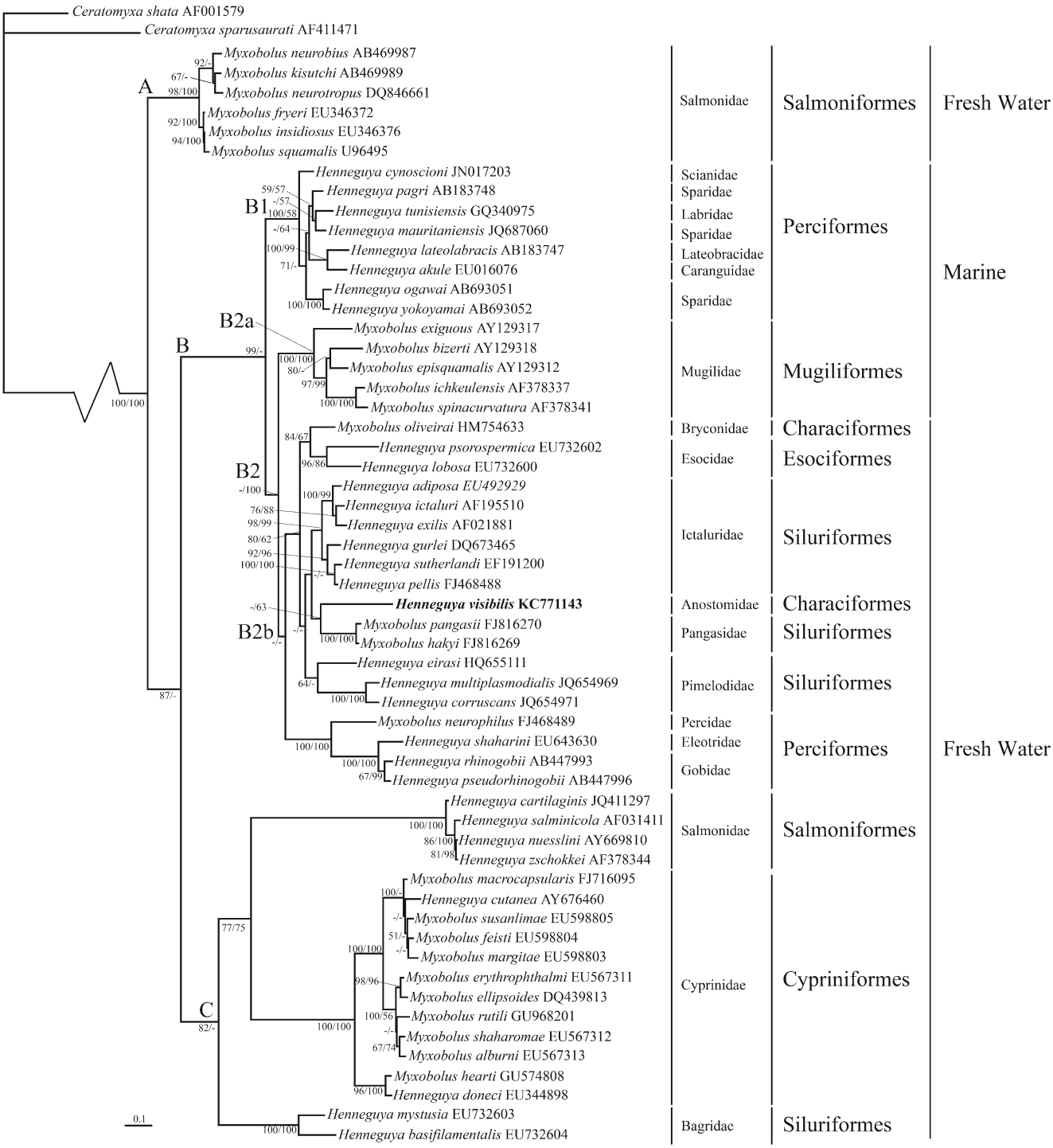

Fig. 10 ML tree showing the relationship between *H. visibilis* n. sp. and other *Henneguya* spp. based on partial 18S rDNA. The *numbers* above the nodes indicate bootstrap confidence levels from ML and maximum parsimony. *Dashes* are shown for values under 50 %

several freshwater fish families; nevertheless, it retained a tendency to group according to the taxonomic affinity of the hosts. *H. visibilis* n. sp. is the first myxosporean parasite species of the Anostomidae family whose 18S rDNA sequence has been analyzed. It appears as a sister branch of the clade composed of two *Myxobolus* spp. parasites of siluriforms of the Pangasiidae family and separated of *M. oliveirai*, which is also a parasite of the characiform, but of the family Bryconidae.

Clade C was composed of *Myxobolus*/*Henneguya* parasite species of cypriniforms, salmoniforms, and two *Henneguya* spp. parasites of siluriforms of the family Bagridae, which

appears off of and even distant from the clade formed by the other parasite species of siluriform fishes.

Our phylogenetic results corroborates the hypothesis of Ferguson et al. (2008), Naldoni et al. (2011), and Adriano et al. (2012), who argued that in phylogenetic studies based on the 18S rDNA gene, myxosporeans tend to group according to host affinity. However, for *H. visibilis* n. sp., the phylogenetic position is still uncertain, and it will only be clarified after 18S rDNA sequences of other myxosporean parasite species of characiform fishes become available.

Acknowledgments This study was supported by the Brazilian fostering agency CNPq (grant number 477658/2010-5). The authors are grateful to the doctoral students Juliana Naldoni, Mateus M. Carriero, and Tiago Milanin for their help in laboratory analyses.

References

Abdel-Ghaffar F, Abdel-Baki AA, Bayoumy EM, Bashtar AR, Al Qurieshy S, Morsey KS, Alghamdy A, Mehlhorn H (2008) Light and electron microscopic study on *Henneguya suprabranchiae* Landsberg, 1987 (Myxozoa: Myxosporea) infecting *Oreochromis niloticus*, a new host record. Parasitol Res 103(3):609–617

Adriano EA, Arana S, Cordeiro NS (2005a) Histology, ultrastructure and prevalence of *Henneguya piaractus* (Myxosporea) infecting the gills of *Piaractus mesopotamicus* (Characidae) cultivated in Brazil. Dis Aquat Org 64(3):229–235

Adriano EA, Arana S, Cordeiro NS (2005b) An ultrastructural and histopathological study of *Henneguya pellucida* n. sp. (Myxosporea: Myxobolidae) infecting *Piaractus mesopotamicus* (Characidae) cultivated in Brazil. Parasite 12(3):221–227

Adriano EA, Arana S, Carriero MM, Naldoni J, Ceccarelli PS, Maia AA (2009) Light, electron microscopy and histopathology of *Myxobolus salminus* n. sp., a parasite of *Salminus brasiliensis* from the Brazilian Pantanal. Vet Parasitol 165(1–2):25–29

Adriano EA, Carriero MM, Maia AAM, Silva MRM, Naldoni J, Ceccarelli PS, Arana S (2012) Phylogenetic and host–parasite relationship analysis of *Henneguya multiplasmodialis* n. sp. infecting *Pseudoplatystoma* spp. in Brazilian Pantanal wetland. Vet Parasitol 185(2–4):110–120

Ali MA, Abdel-Baki AS, Sakran T, Entzeroth R, Abdel-Ghaffar F (2007) *Myxobolus lubati* n. sp. (Myxosporea: Myxobolidae), a new parasite of haffara seabream *Rhabdosargus haffara* (Forsskal, 1775), Red Sea, Egypt: a light and transmission electron microscopy. Parasitol Res 100(4):819–827

Altschul SF, Madden TL, Schaffer AA, Zhang JH, Zhang Z, Miller W, Lipman DJ (1997) Gapped BLAST and PSI-BLAST: a new generation of protein database search programs. Nucleic Acids Res 25(17):3389–3402

Azevedo C, Casal G, Matos P, Matos E (2008) A new species of Myxozoa, *Henneguya rondoni* n. sp. (Myxozoa), from the peripheral nervous system of the Amazonian fish, *Gymnorhamphichthys rondoni* (Teleostei). J Eukaryot Microbiol 55(3):229–234

Azevedo C, Casal G, Mendonca I, Matos E (2009) Fine structure of *Henneguya hemiodopsis* sp. n. (Myxozoa), a parasite of the gills of the Brazilian teleostean fish *Hemiodopsis microlepes* (Hemiodontidae). Mem Inst Oswaldo Cruz 104(7):975–979

Azevedo C, Casal G, Matos P, Alves A, Matos E (2011) *Henneguya torpedo* sp. nov. (Myxozoa), a parasite from the nervous system of the Amazonian teleost *Brachyhypopomus pinnicaudatus* (Hypopomidae). Dis Aquat Org 93(3):235–242

Barassa B, Adriano EA, Cordeiro NS, Arana S, Ceccarelli PS (2012) Morphology and host–parasite interaction of *Henneguya azevedoi* n. sp., parasite of gills of *Leporinus obtusidens* from Mogi-Guacu River, Brazil. Parasitol Res 110(2):887–894

Barta JR, Martin DS, Liberator PA, Dashkevicz M, Anderson JW, Feighner SD, Elbrecht A, Perkins-Barrow A, Jenkins MC, Danforth HD, Ruff MD, Profous-Juchelka H (1997) Phylogenetic relationships among eight Eimeria species infecting domestic fowl inferred using complete small subunit ribosomal DNA sequences. J Parasitol 83(2):262–271

Bartholomew JL, Atkinson SD, Hallett SL, Lowenstine LJ, Garner MM, Gardiner CH, Rideout BA, Keel MK, Brown JD (2008) Myxozoan parasitism in waterfowl. Int J Parasitol 38(10):1199–1207

Casal G, Matos E, Azevedo C (2003) Light and electron microscopic study of the myxosporean, *Henneguya friderici* n. sp. from the *Amazonian teleostean* fish, *Leporinus friderici*. Parasitology 126: 313–319

Current WL, Janovy J Jr (1976) Ultrastructure of interlamellar *Henneguya exilis* in the channel catfish. J Parasitol 62(6):975–981

Diamant A, Whipps CM, Kent ML (2004) A new species of *Sphaeromyxa* (Myxosporea: Sphaeromyxina: Sphaeromyxidae) in devil firefish, *Pterois miles* (Scorpaenidae), from the northern Red Sea: morphology, ultrastructure, and phylogeny. J Parasitol 90(6):1434–1442

Easy RH, Johnson SC, Cone DK (2005) Morphological and molecular comparison of *Myxobolus procerus* (Kudo, 1934) and *M. intramusculi* n. sp. (Myxozoa) parasitising muscles of the trout-perch *Percopsis omiscomaycus*. Syst Parasitol 61(2):115–122

Eiras JC (2002) Synopsis of the species of the genus *Henneguya* Thélohan, 1892 (Myxozoa: Myxosporea: Myxobolidae). Syst Parasitol 52(1):43–54

Eiras JC, Adriano EA (2012) A checklist of new species of *Henneguya* Thélohan, 1892 (Myxozoa: Myxosporea, Myxobolidae) described between 2002 and 2012. Syst Parasitol 83(2):95–104

Eiras JC, Malta JC, Varela A, Pavanelli GC (2004) *Henneguya schizodon* n. sp. (Myxozoa, Myxobolidae), a parasite of the Amazonian teleost fish *Schizodon fasciatus* (Characiformes, Anostomidae). Parasite 11(2):169–173

Eiras JC, Takemoto RM, Pavanelli GC (2008) *Henneguya caudicula* n. sp. (Myxozoa, Myxobolidae), a parasite of *Leporinus lacustris* (Osteichthyes, Anostomidae) from the high Paraná River, Brazil, with a revision of *Henneguya* spp. infecting South American fish. Acta Protozool 47(2):149–154

Eiras JC, Takemoto RM, Pavanelli GC (2009) *Henneguya corruscans* n. sp. (Myxozoa, Myxosporea, Myxobolidae), a parasite of *Pseudoplatystoma corruscans* (Osteichthyes, Pimelodidae) from the Paraná River, Brazil: a morphological and morphometric study. Vet Parasitol 159(2):154–158

El-Mansy A, Bashtar AR (2002) Histopathological and ultrastructural studies of *Henneguya suprabranchiae* Landsberg, 1987 (Myxosporea: Myxobolidae) parasitizing the suprabranchial organ of the freshwater catfish *Clarias gariepinus* Burchell, 1822 in Egypt. Parasitol Res 88(7):617–626

Feist SW, Longshaw M (2006) Phylum Myxozoa. In: Woo PTK (ed) Fish diseases and disorders: protozoan and metazoan infections. CABI, Wallingford, pp 230–296

Ferguson JA, Atkinson SD, Whipps CM, Kent ML (2008) Molecular and morphological analysis of *Myxobolus* spp. of salmonid fishes with the description of a new *Myxobolus* species. J Parasitol 94(6):1322–1334. doi:10.1645/GE-1606.1

Fiala I (2006) The phylogeny of Myxosporea (Myxozoa) based on small subunit ribosomal RNA gene analysis. Int J Parasitol 36(14):1521–1534

Fleurance R, Sauvegrain C, Marques A, Le Breton A, Guereaud C, Cherel Y, Wyers M (2008) Histopathological changes caused by

Enteromyxum leei infection in farmed sea bream *Sparus aurata*. Dis Aquat Org 79(3):219–228

Froese R, Pauly D (2012) FishBase. World Wide Web electronic publication, version (09/2012). www.fishbase.org. Accessed 29 Jan 2013

Guindon S, Dufayard JF, Lefort V, Anisimova M, Hordijk W, Gascuel O (2010) New algorithms and methods to estimate maximum-likelihood phylogenies: assessing the performance of PhyML 3.0. Syst Biol 59(3):307–321

Hall TA (1999) BioEdit: a user-friendly biological sequence alignment editor and analysis program for Windows 95/98/NT. Nucleic Acids Symp Ser 41:95–98

Hubert N, Renno JF (2006) Historical biogeography of South American freshwater fishes. J Biogeogr 33(8):1414–1436

Iwanowicz LR, Iwanowicz DD, Pote LM, Blazer VS, Schill WB (2008) Morphology and 18S rDNA of *Henneguya gurlei* (Myxosporea) from *Ameiurus nebulosus* (Siluriformes) in North Carolina. J Parasitol 94(1):46–57

Khlifa S, Miller TL, Adlard RD, Faye N, Sasal P (2012) *Henneguya mauritaniensis* n. sp. (Myxozoa) from the arterial bulb of *Pagrus caeruleostictus* (Valenciennes, 1830) off Mauritania. Parasitol Res 111(3):1287–1294

Liu Y, Whipps CM, Gu ZM, Zeng LB (2010) *Myxobolus turpisrotundus* (Myxosporea: Bivalvulida) spores with caudal appendages: investigating the validity of the genus *Henneguya* with morphological and molecular evidence. Parasitol Res 107(3):699–706

Lom J, Arthur JR (1989) A guideline for the preparation of species description in Myxosporea. J Fish Dis 12:151–156

Lom J, Dykova I (2006) Myxozoan genera: definition and notes on taxonomy, life-cycle terminology and pathogenic species. Folia Parasitol 53(1):1–36

Martins ML, de Souza VN, de Moraes JR, de Moraes FR (1999) Gill infection of *Leporinus macrocephalus* Garavello & Britski, 1988 (Osteichthyes: Anostomidae) by *Henneguya leporinicola* n. sp. (Myxozoa: Myxobolidae). Description, histopathology and treatment. Rev Bras Biol 59(3):527–534

Milanin T, Eiras JC, Arana S, Maia AA, Alves AL, Silva MR, Carriero MM, Ceccarelli PS, Adriano EA (2010) Phylogeny, ultrastructure, histopathology and prevalence of *Myxobolus oliveirai* sp. nov., a parasite of *Brycon hilarii* (Characidae) in the Pantanal wetland, Brazil. Mem Inst Oswaldo Cruz 105(6):762–769

Molnár K (1998) Taxonomic problems, seasonality and histopathology of *Henneguya creplini* (Myxosporea) infection of the pikeperch *Stizostedion lucioperca* in Lake Balaton. Folia Parasitol 45(4): 261–269

Molnár M (2002) Site preference of myxosporean spp. on the fins of some Hungarian fish species. Dis Aquat Org 52(2):123–128

Molnár K, Eszterbauer E, Szekely C, Dan A, Harrach B (2002) Morphological and molecular biological studies on intramuscular *Myxobolus* spp. of cyprinid fish. J Fish Dis 25(11):643–652

Molnár K, Marton S, Eszterbauer E, Szekely C (2006) Comparative morphological and molecular studies on *Myxobolus* spp. infecting chub from the river Danube, Hungary, and description of *M. muellericus* sp. n. Dis Aquat Org 73(1):49–61

Morris DJ (2010) Cell formation by myxozoan species is not explained by dogma. Proc R Soc B 277:2565–2570

Naldoni J, Arana S, Maia AA, Silva MR, Carriero MM, Ceccarelli PS, Tavares LE, Adriano EA (2011) Host–parasite–environment relationship, morphology and molecular analyses of *Henneguya eirasi* n. sp. parasite of two wild *Pseudoplatystoma* spp. in Pantanal Wetland, Brazil. Vet Parasitol 177(3–4):247–255

Nemeczek A (1926) Beitrage zur Kenntnis der Myxosporidien fauna Brasiliens. Arch Protistenkd 54:137–149

Posada D (2008) jModelTest: phylogenetic model averaging. Mol Biol Evol 25(7):1253–1256

Rambaut A (2009) Molecular evolution, phylogenetics and epidemiology. FigTree v1.3.1. http://tree.bio.ed.ac.uk/software/figtree/. Accessed 5 Feb 2012

Rosenberg MS, Kumar S (2001) Incomplete taxon sampling is not a problem for phylogenetic inference. Proc Natl Acad Sci U S A 98(19):10751–10756

Santos GO (2000) Aspectos importantes para a piscicultura do gênero *Leporinus* Spix, 1829 uma revisão. Pesq Agrop Gaúcha 6:151–156

Sitja-Bobadilla A (2008) Fish immune response to Myxozoan parasites. Parasite 15(3):420–425

Swofford DL (2003) PAUP*. Phylogenetic Analysis Using Parsimony (*and Other Methods). Sinauer Associates, Sunderland

Tamura K, Peterson D, Peterson N, Stecher G, Nei M, Kumar S (2011) MEGA5: Molecular Evolutionary Genetics Analysis using maximum likelihood, evolutionary distance, and maximum parsimony methods. Mol Biol Evol 28(10):2731–2739

Thompson JD, Gibson TJ, Plewniak F, Jeanmougin F, Higgins DG (1997) The CLUSTAL_X windows interface: flexible strategies for multiple sequence alignment aided by quality analysis tools. Nucleic Acids Res 25(24):4876–4882